25GHz Hybrid Silicon Mach-Zehnder Modulator using High-Speed Push-Pull Slotline Design

Hui-Wen Chen, Jonathan D. Peters and John E. Bowers
Department of Electrical and Computer Engineering, University of California Santa Barbara, CA 93106, USA
E-mail:hwchen@ece.ucsb.edu

Abstract: We demonstrate a hybrid silicon Mach-Zehnder modulator having a voltage-length product of 2.4 V-mm and chirp parameter of -0.75. This modulator also has a modulation bandwidth of 25 GHz.
OCIS codes: (000.0000) General; 250.4110 Modulators www.opticsinfobase.org/submit/ocis.]

1. Introduction

Recent efforts in silicon photonics have focused on developing a wide range of optical components that can be integrated on a single platform [1]. A lot of work has centered on modulators as they are crucial for the generation and transmission of high-speed signals such that increasing demands on data capacity can be satisfied. To be able to efficiently send information at high frequencies, modulators with large optical bandwidth, high-speed operation and good modulation efficiency are required. Modulators based on a Mach-Zehnder interferometer architecture are of particular interest because they satisfy several of the aforementioned criteria. The optical bandwidth of a Mach-Zehnder modulator (MZM) can be close to a 100 nm [2-4] while that of a ring resonator structure is typically a few nm [5] and that of an electroabsorption modulator (EAM) is less than 30 nm [6, 7]. Having a wide optical bandwidth is especially useful for tunable integrated transmitters. Pure silicon based modulators have had to trade modulation bandwidth for modulation efficiency due to the intrinsic properties of the material (Si). Modulators fabricated on a hybrid III-V/ Silicon platform do not suffer from these limitations and as such offer a way to realize compact, efficient and high bandwidth modulators. Previously, MZM on the hybrid silicon platform have been demonstrated to have a bandwidth of 15 GHz, large signal modulation up to 25 Gb/s with 10 dB extinction ratio (ER) and voltage length products of 2.4 V-mm [8]. Here we report on an improved electrode design with a bandwidth of 25GHz. We analyze and report on the negative chirp of these modulators, which can be useful for extending the reach of a transmitter.

2. Device Design

The MZM was fabricated on the hybrid silicon platform [9] such that the modulator efficiency can be increased compared to pure silicon modulators by utilizing III-V material that is wafer bonded using a low temperature bonding technique [10]. To have a good balance between modulation efficiency and bandwidth, this modulator uses doped quantum wells to introduce index change via the carrier depletion effect, where the modulation bandwidth is limited by device resistance and capacitance rather than carrier lifetime. The PL of the quantum well is designed to be at 1460 nm so that it is far enough from the operating wavelength to avoid unwanted losses. The hybrid silicon MZM has a multimode interference (MMI) splitter and combiner at the input and output respectively. to split the incoming signal and combine the modulated light. All the III-V material is removed during the process except for the region marked in orange in Fig. 1(a) (hybrid section) to reduce propagation loss. Two silicon/III-V tapers are utilized between the silicon and hybrid sections to reduce reflection and increase coupling efficiency.

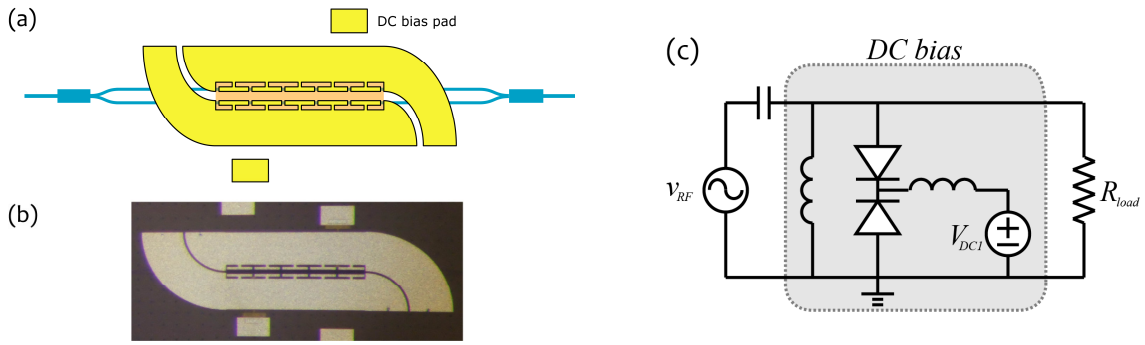

Fig. 1. (a) Top Schematic of a 500 μm MZM (b) Optical image of a fabricated device (c) Equivalent circuit of push-pull slotline design

In order to achieve push-pull operation while keep both arms of the MZM reverse biased, a slotline design is adopted rather than a coplanar waveguide (CPW) for the traveling wave electrode. An equivalent circuit for this electrode design is shown in Fig. 1(c) where each arm of the MZM is treated as a diode. As can been seen, both arms can be reverse biased by adjusting V_{DC1} via a DC pad connected to the common ground. The RF signal, on the other hand, is applied to the p side of the diodes, and consequently the voltage drop on each diode will be $V_{DC1} \pm v_{RF}$. This differential RF drive signal usually results in very small or negative chirp, which counterbalances fiber dispersion in long haul transmission systems and decreases power penalty. Moreover, with such a push-pull structure, the modulation bandwidth can also be enhanced since the device capacitance is reduced by a factor of two by series connecting two diodes. In addition to conventional traveling wave electrode design (TWE), a capacitively loaded (CL) TWE [8, 11, 12] is utilized on this MZM to reduce electrical propagation loss, increase device impedance, and reduce velocity mismatch between the traveling wave optical and electrical signals.

3. Experimental Results

To explore the DC characteristics of the MZM, lensed fibers are used to couple the light in and out of a silicon waveguide. The normalized transmission as a function of reverse bias for two devices is shown in Fig. 2. As can be seen, the V_π of a 500 μm long modulators is 4.8 V, which results in a voltage length product of 2.4 V-mm. The ER is 19.5 dB and optical loss of the hybrid section is 3 dB/mm. The second transmission peak is about 3 dB less than the first one due to the power imbalance between two arms at higher bias voltage, where the quantum confined Stark effect (QCSE) starts to contribute to index change and introduce additional loss.

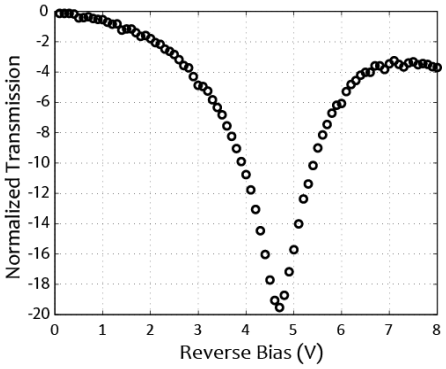

Fig. 2. Normalized transmission of a 500 μm MZM at 1550nm

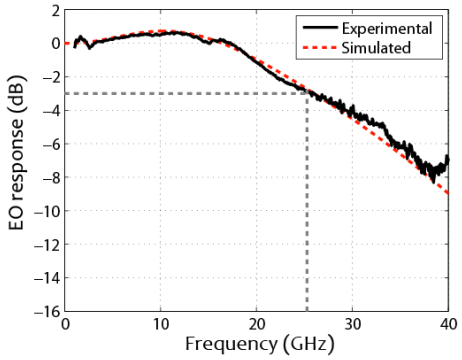

Fig. 3. Modulation bandwidth of a 500 μm MZM at -3 V bias

The high speed performance of this hybrid silicon modulator is also of great interest. Fundamental parameters were first extracted by measuring all four S parameter of a 500 μm modulator using an Agilent N4373C Lightwave Component Analyzer (LCA) with -3 V reverse bias. The experimental data shows that the modulator has 35 Ω characteristic impedance. Next, the EO response was measured with a 25 Ω termination to eliminate reflection from the end of transmission line. The experimental result in Fig. 3 shows a modulation bandwidth of 25 GHz, which suggests that this device has the potential for 40 Gb/s NRZ operation. A simulated EO response is shown in Fig. 3 with the parameters extracted from the S parameter measurement, together with a 6 Ω series resistance and a 0.62 pF device capacitance. As can be seen, the simulation agrees well with the experiment.

In addition to the modulation bandwidth, chirp is one of the important metrics for data transmission. The chirp parameter of a MZM can be expressed approximately in terms of the phase change in each arm ($\Delta\phi_2$ and $\Delta\phi_1$) as [13]:

$$\alpha = \frac{\Delta\phi_1 + \Delta\phi_2}{\Delta\phi_1 - \Delta\phi_2} \tag{1}$$

With the push-pull configuration, the phase changes in the two arms have the same amplitude but are out of phase ($\Delta\phi_2 = -\Delta\phi_1$) such that chirp-free modulation can be achieved as shown in Eq. (1). In reality, however, the amplitudes of phase change in two arms are usually not identical because the electrorefraction effect is bias dependent. Therefore, an ideal zero chirp condition can only be realized if the modulation effect is perfectly linear.

The small signal chirp parameter can be obtained by measuring the EO response by inserting a dispersive fiber between the modulator and the LCA [14]. The interaction between fiber dispersion and modulator chirp results in resonance dips in the spectrum as shown in Fig. 3 (a). The relationship between the resonance points and the chirp can be written as [14]:

$$f_u^2 L = \frac{c_0}{2D\lambda^2}\left(1 + 2u - \frac{2}{\pi}\arctan(\alpha)\right) \tag{2}$$

,where f_u is the *u*th order of resonance, c_0 is the speed of light, D is the fiber dispersion, λ is the wavelength, and α is the chirp. By fitting the experimental resonance points into Eq. (2), the chirp under different biases can be calculated and the result is shown in Fig. 3(b). It indicates that the chirp is around -0.75 over a 5 V range. This negative chirp can counteract dispersion and consequently reduce the power penalty for long-haul data transmission applications. We are currently working on the BER measurement.

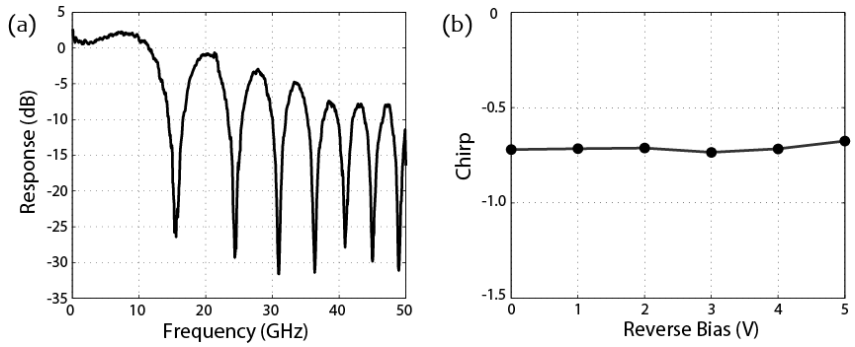

Fig. 3. (a) EO response with 28 km SMF between the LCA and the MZM. (b) Chirp parameters at different bias condition.

4. Summary

We successfully demonstrate a hybrid silicon MZM with a voltage length products of 2.4 V-mm and ER of 19.5 dB. The modulation bandwidth is 25 GHz and the modulator has a chirp parameter of -0.75 over a 5 V range. Such a modulator has the potential to support large signal modulation at 40 Gb/s as well as have a low power penalty.

5. Acknowledgements

The authors thank Brain Thibeault and Ying-hao Kuo for process advice. The authors also thank Yongbo Tang, Jae Shin, Anand Ramaswamy, and Molly Piels for useful suggestions on device designing and testing. A portion of this work was done in the UCSB nanofabrication facility, part of the NSF funded NNIN network. This work was supported by Rockwell Collins.

6. References

[1] H. Park, et al., "Device and Integration Technology for Silicon Photonic Transmitters," *to be published in J. Selected Topics in Quantum Electronics,* (2010).
[2] A. Liu, et al., "High-speed optical modulation based on carrier depletion in a silicon waveguide," *Opt Express* **15**, 660-668 (2007).
[3] H.-W. Chen, et al, "A Hybrid Silicon–AlGaInAs Phase Modulator,"*IEEE Photon. Tech. Lett.*, **20**, 1920-1922 (2008)
[4] J. Van Campenout, et al., "Low-power, 2×2 silicon electro-optic switch with 110-nm bandwidth for broadband reconfigurable optical networks," *Opt Express* **17**, 24020-24029 (2009).
[5] Q. Xu, et al., "Micrometer-scale silicon electrooptic modulator," *Nature* **435**, 325-327 (2005).
[6] Y.-H. Kuo, et al, "High speed hybrid silicon evanescent electroabsorption modulator," *Opt. Express* **16**, 9936-9941 (2008).
[7] J. Liu, et al., "Waveguide-integrated, ultralow-energy GeSi electro-absorption modulators," *Nature Photonics* **2**, 433-437 (2008).
[8] H.-W. Chen, et al, "25Gb/s hybrid silicon switch using a capacitively loaded traveling wave electrode," *Opt Express* **18**, 1070-1075 (2010).
[9] A. W. Fang, et al, "Electrically pumped hybrid AlGaInAs-silicon evanescent laser," *Opt. Express* **14**, 9203-29210 (2006).
[10] D. Liang, *et al.*, "Highly efficient vertical outgassing channels for low-temperature InP-to-silicon direct wafer bonding on the silicon-on-insulator substrate," *J. Vac. Sci. Tech.*, **26**, 1560-1568 (2008).
[11] J. Shin, et al.,"Novel T-rail electrodes for substrate removed low-voltage high-speed GaAs/AlGaAs electrooptic modulators," *IEEE Trans. Microwave Theory Tech.*, **53**, 636-643 (2005).
[12] S. Akiyama, "Wide-Wavelength-Band (30 nm) 10 Gb/s Operation of InP-Based Mach-Zehnder Modulator With Constant Driving Voltage of 2 Vpp," *IEEE Photon. Tech. Lett.*, **17**, 1408 (2005).
[13] J. C. Cartledge, et al., "Theoretical Performance of 10 Gb/s lightwave systems using a III-V semiconductor Mach-Zehnder modulator," *IEEE Photon. Tech. Lett.*, **6**, 282-284 (1994).
[14] F. Devaux, et al., "Simple Measurement of fiber Dispersion and of Chirp Parameter of Intensity Modulated Light Emitter,"*IEEE Photon. Tech. Lett.*, **11**, 1937-1940 (1993).